



**HAL**  
open science

## Radio Capacity Improvement with HSPA+ Dual-Cell

Thomas Bonald, Salah Eddine Elayoubi, Ammar El Falou, Jean-Baptiste Landre

► **To cite this version:**

Thomas Bonald, Salah Eddine Elayoubi, Ammar El Falou, Jean-Baptiste Landre. Radio Capacity Improvement with HSPA+ Dual-Cell. ICC, Jun 2011, Kyoto, Japan. pp.1 - 6, 10.1109/icc.2011.5963497 . hal-01112984

**HAL Id: hal-01112984**

**<https://imt.hal.science/hal-01112984>**

Submitted on 4 Feb 2015

**HAL** is a multi-disciplinary open access archive for the deposit and dissemination of scientific research documents, whether they are published or not. The documents may come from teaching and research institutions in France or abroad, or from public or private research centers.

L'archive ouverte pluridisciplinaire **HAL**, est destinée au dépôt et à la diffusion de documents scientifiques de niveau recherche, publiés ou non, émanant des établissements d'enseignement et de recherche français ou étrangers, des laboratoires publics ou privés.

# Radio capacity improvement with HSPA+ dual-cell

T. Bonald, S.E. Elayoubi, A. El Falou, J.B. Landre

Orange labs  
Issy-Les-Moulineaux, France

**Abstract** –This paper studies the radio capacity improvement provided by an HSPA+ key feature, dual-cell, combined with MIMO. The proposed method combines drive test measurements, link-level simulations, and a queuing theory-based statistical capacity model, thereby providing a reliable estimate of the network radio capacity. Simulation results show that dual cell combined with MIMO and non-linear receivers using Successive Interference Cancellation (SIC) significantly increases network radio capacity. These results confirm that HSPA networks evolutions are promising.

## I. INTRODUCTION

3G wireless technology has kept improving since the first releases of the 3G standards. Each new release of 3GPP specification comes with new features that bring progress both to consumers and network operators. 3GPP Release 7 specifies HSPA+, which introduces several significant improvements over HSDPA Release 5 [1], such as Continuous Packet Connectivity (CPC), 64QAM modulation and MIMO [2]. In Release 8, HSPA dual-cell aggregates two adjacent carriers, thanks to a joint scheduling scheme. In Release 9, dual-cell and MIMO can be combined [3]. The advantage of dual-cell is that it improves the user throughput for a given load, for any location in the cell, even at cell edge. Moreover, it is expected to bring high radio capacity gains. This feature is therefore held as the most important feature of HSPA+ so far. The reason is that operators are facing an important increase of data traffic, which they may not be able to cope with in the medium term. They obviously pay a high attention to HSPA features that improve spectral efficiency since this can delay the need for new spectrum, and also delay the rollout of new LTE networks that have better spectrum efficiency.

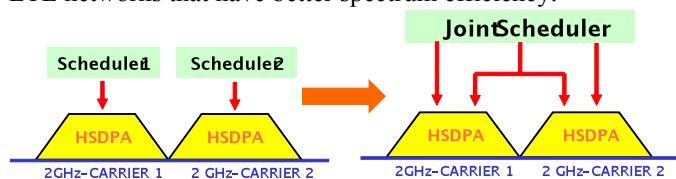


Figure 1. From single-cell scheduling to dual-cell in 3GPP R8

The purpose of this paper is to assess the capacity gain provided by HSPA dual-cell feature, first for Release 8 compliant networks (i.e. without MIMO), and second for Release 9 compliant devices (i.e. when dual-cell and MIMO are combined). In [4], we proposed a throughput prediction method that combines drive test measurements made with a scanner equipment, and link-level simulations results. This method is able to give accurate HSPA throughput predictions for any HSPA device. We show in this paper how to combine these realistic throughput predictions with queuing theory

methods in order to derive the capacity gains for streaming and data services. In particular, we extend the theory developed in [5] for single carrier systems to the dual-cell case; the main difficulty comes from the mix between legacy, single-carrier devices and HSPA+ dual cell ones.

The capacity gain from dual-cell is known to come from frequency diversity, higher multi-user diversity, and trunking effect due to statistical multiplexing. A few previous works have started the evaluation. In [6], the gains from frequency diversity and higher multi-user diversity have been evaluated; these gains are used as inputs for our capacity model. Simulation results are provided in [7] and [8] for full-buffer traffic. However, the trunking gain cannot be observed for full buffer traffic, as explained in [6], and has not yet been evaluated. This paper gives for the first time an evaluation of the trunking gain for elastic data traffic and streaming traffic, and brings a complete model for the HSPA+ dual-cell feature.

This paper is organized as follows. Section II presents the link level modeling and throughput predictions. We discuss in section III the methodology to estimate cell radio capacity. The obtained results are shown and discussed in section IV.

## II. USER THROUGHPUT EVALUATION METHODOLOGY

### A. Link level modelling and outputs

The link-layer modeling methodology is detailed in [4]. It consists of four steps:

- Estimate of SINR at the receiver's output.
- Selection of the modulation and coding scheme (MCS) combination that maximizes the throughput.
- Packet viability assessment according to FER lookup table.
- HARQ retransmission in case of packet error. Chase combining with a maximum of four retransmissions is modeled.

Each device category is simulated with the most probable receiver based on a market survey: Rake receivers are used for 1.4Mbps-capable devices. Linear minimum mean squared error (LMMSE) receivers, combined with receive diversity are used from 3.6 to 21 Mbps-capable devices, as well as for dual-cell devices [6]. LMMSE, combined with successive interference cancellation (SIC) receiver, is used for MIMO devices [10] [11].

### B. Single-user throughput evaluation

Single-user throughput is calculated with the method defined in [4]. This method combines the accuracy of field measurements on a live network with an estimate of the performance of all HSDPA devices. There are two steps in the

calculations. First, an estimate of the average HS-DSCH Signal to Noise Ratio (SNR) is calculated using CPICH Ec/I0 and CPICH RSCP figures measured by a scanner equipment during drive tests. Second, HSDPA throughput for this average SNR is obtained from lookup tables that contain the results of the link-level simulations. A “simulated” HSDPA drive test is obtained at the end, with an estimate of the throughput that would have been experienced by an HSDPA device for each measurement sample. As the scrambling code of the serving cell is available for each sample, the measurements relative to each of the cells can then be extracted, and calculations can be made cell by cell.

This method can be applied for all HSDPA device categories, for all the receivers' type (rake, LMMSE, SIC-LMMSE ...), on the same drive test. This comes with a huge improvement over classical system simulations that are based on hexagonal cells modeling, and statistical propagation models such as Cost-Hata [12], which is quite far from real-life conditions. Measured Ec/I0 and RSCP figures are much more accurate than predicted values.

### III. RADIO CAPACITY

HSDPA radio capacity calculation is not as straightforward as one might expect. The common method consists in defining the cell capacity as the served throughput for a given number of users in the cell, using a static simulator ([8] [13]). There are however one key drawback in this method: it does not consider the statistical behavior of the traffic demand. Indeed, in a real network, the number of users in the cell keeps changing, and the activity of each user is not constant over time. We usually refer to these models as “Erlang-like”, since they model the statistical behavior of the traffic, in a similar way as the Erlang B law does.

#### A. Elastic traffic

##### 1) Single Carrier

We start with the simplest case, where only legacy terminals are served by the cell. In the absence of load balancing mechanisms, the traffic demand, denoted by  $A$ , can be considered as equally split between the two operating carriers. The capacity of a single HSDPA carrier has been addressed in [5] for a circular cell case. In this paper, we show how to apply this model on drive test predictions.

Let  $C$  be the harmonic average of the single-user throughput, obtained from the drive test simulations:

$$C = \left[ \frac{1}{|S|} \sum_{u \in S} \frac{1}{T_{alone}(u)} \right]^{-1} \quad (1)$$

where  $S$  is the set of points considered in the studied cell and  $|S|$  its cardinality.  $T_{alone}(u)$  is the throughput predicted by the drive test simulations in position  $u$ .

To calculate user throughput, we use a Processor Sharing (PS) queue that gives the distribution of users in the cell. Defining the carrier load  $\rho = (A/2)/C$ , the probability that the number of users in the cell  $M$  is equal to  $m$ , is:

$$\Pr[M = m] = \rho^m (1 - \rho) \quad (2)$$

Based on this probability distribution and on the single-user throughput over the cell, we can characterize the user perceived QoS, in terms of average throughput and throughput percentiles.

First, the probability that a HSDPA user, located at position  $u$  in the cell, has an average flow throughput equal to  $t(u|m) = T_{alone}(u)/m$ , knowing that there are  $m$  active users in the cell, is given by:

$$\Pr[t(u|m)] = \frac{m \Pr[M = m]}{\sum_n n \Pr[M = n]} = \frac{m \rho^m (1 - \rho)}{E[M]} \quad (3)$$

where  $E[M] = \frac{\rho}{1 - \rho}$  is the average number of users in the cell.

Thus, the average user flow throughput over the cell is:

$$\bar{T} = E_{u \in S} \left[ \sum_{m \geq 1} t(u|m) \Pr[t(u|m)] \right] = \frac{1 - \rho}{|S|} \sum_{u \in S} T_{alone}(u) \quad (4)$$

If a target throughput  $T_{min}$  is fixed for HSDPA users, the probability of achieving this target is equal to:

$$\Pr[T \geq T_{min}] = \frac{1}{|S|} \sum_{u \in S} \sum_{m \leq \frac{T_{alone}(u)}{T_{min}}} \frac{m \rho^m (1 - \rho)}{E[M]} \quad (5)$$

##### 2) Dual Carrier

New HSDPA UE categories (21-24) have been introduced to support the DC HSDPA feature. They can simultaneously use the two available carriers in the cell, as described in Figure 1. This doubles the stand-alone throughput at each point of the cell and its harmonic average throughput. Thus, the cell load

becomes:  $\rho = \frac{A}{2C}$ . This leads to the same probability

distribution function and a doubling in the average flow throughput of equation (4).

However, the percentiles of the throughput are not doubled, as the probability of achieving a throughput target can be calculated, as above, by:

$$\Pr[T \geq T_{min}] = \frac{1}{|S|} \sum_{u \in S} \sum_{m \leq \frac{2T_{alone}(u)}{T_{min}}} \frac{m \rho^m (1 - \rho)}{E[M]} \quad (6)$$

##### 3) Mix of single and dual carrier users

Even if all new UE categories are DC-compliant, they will coexist with legacy SC users. Therefore, the available  $2 \times 5$  MHz carriers are used to serve both SC and DC users simultaneously.

The cell can then be modelled as three queues: two queues of capacity  $C$  each receiving the single carrier traffic, and one queue of capacity  $2C$  receiving all the traffic (see Figure 2).

We denote by class 1 the legacy traffic carried by one carrier; by class 2 the legacy traffic carried by the other carrier and by class 3 the dual carrier traffic. The network state is defined by the vector  $\mathbf{x} = (x_1, x_2, x_3)$  where  $x_c$  is the number of class- $c$  users in progress. According to [14], the steady-state

probabilities describing the evolution of the number of calls of each class,  $\mathbf{x} = (x_1, x_2, x_3)$  are calculated by:

$$\pi(\mathbf{x}) = \frac{1}{G} \Phi(\mathbf{x}) \rho_1^{x_1} \rho_2^{x_2} \rho_3^{x_3} \quad (7)$$

where  $\rho_c$  is the offered load of class  $c$  flow ( $\rho_3 = \frac{A_{DC}}{2C}$  and

$$\rho_1 = \rho_2 = \frac{A_{SC}}{2C}) \text{ and } G = \sum_{\mathbf{x}} \Phi(\mathbf{x}) \rho_1^{x_1} \rho_2^{x_2} \rho_3^{x_3}.$$

The function  $\Phi$  describes the balanced allocation between carriers and can be calculated recursively by:

$$\Phi(\mathbf{x}) = \begin{cases} 0, & x_c < 0, \forall c \in \{1,2,3\} \\ 1, & x_c = 0, \forall c \in \{1,2,3\} \\ \max \left[ \frac{\Phi(\mathbf{x} - e_1)}{C}, \frac{\Phi(\mathbf{x} - e_2)}{C}, \sum_{c=1}^3 \frac{\Phi(\mathbf{x} - e_c)}{C} \right] & \text{otherwise} \end{cases} \quad (8)$$

where  $e_c$  is a  $(3 \times 1)$  vector with 1 in component  $c$  and 0 elsewhere. The resources allocated to the different classes is:

$$\varphi_c(\mathbf{x}) = \frac{\Phi(\mathbf{x} - e_c)}{\Phi(\mathbf{x})} \quad (9)$$

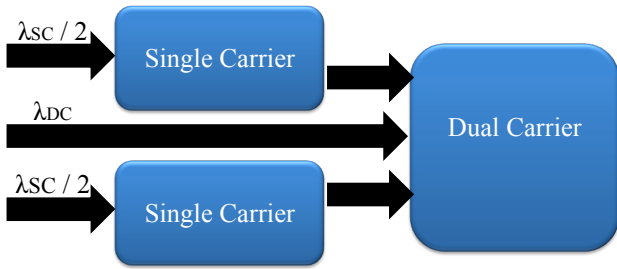


Figure 2. Both SC and DC users coexist in the cell.

The average flow throughput of a class- $c$  user at position  $u$  is:

$$\bar{T}_c(u) = \begin{cases} \frac{T_{alone}(u) \rho_c}{E[x_c]} & c \in \{1,2\} \\ \frac{2T_{alone}(u) \rho_3}{E[x_3]} & c = 3 \end{cases} \quad (10)$$

And the probability of attaining the target throughput  $T_{min}$  for class- $c$  calls is equal to:

$$\Pr[T_c \geq T_{min}] = \frac{1}{|S|} \sum_{u \in S} \sum_{\mathbf{x}: \frac{T_{alone}(u) \varphi_c(\mathbf{x})}{x_c} > T_{min}} \frac{x_c \pi(\mathbf{x})}{E[x_c]} \quad (11)$$

### B. Streaming traffic

Unlike elastic traffic whose QoS is expressed by a throughput performance, streaming calls require a guaranteed throughput  $T^s$  over time; their QoS is thus expressed by a blocking rate.

#### 1) Single Carrier

Let  $m_u$  be the number of streaming users in position  $u$  of the cell. The Call Admission Control (CAC) condition ensuring that the required throughput is guaranteed for all users is:

$$\sum_{u \in S} m_u \frac{T^s}{T_{alone}(u)} \leq 1 \quad (12)$$

Indeed, a call with a stand-alone throughput equal to  $T_{alone}(u)$  occupies all the carrier resources for a time proportion equal to  $\frac{T^s}{T_{alone}(u)}$ . The capacity of the system can then be analysed

using a classical multi-Erlang approach, where the state of the system is defined by the vector  $\mathbf{m} = (m_u, u \in S)$  describing the number of calls of different radio conditions and the CAC condition becomes  $\mathbf{m} \cdot \mathbf{c} \leq 1$ , where  $\mathbf{c} = (\frac{T^s}{T_{alone}(u)}, u \in S)$

is the vector of required throughputs.

The steady-state probabilities are then calculated by:

$$\pi(\mathbf{m}) = \frac{\prod_{u \in S} \left( \frac{1}{|S|} \frac{E}{2} \right)^{m_u} \frac{1}{m_u!}}{\sum_{\mathbf{m}: \mathbf{m} \cdot \mathbf{c} \leq 1} \prod_{v \in S} \left( \frac{1}{|S|} \frac{E}{2} \right)^{m_v} \frac{1}{m_v!}} \quad (13)$$

where  $E$  is the traffic in Erlang. The blocking probability is:

$$b^s = \sum_{u \in S} p_n \sum_{\mathbf{m}: (\mathbf{m} + e_n) \cdot \mathbf{c} > 1} \pi(\mathbf{m}) \quad (14)$$

However, as there are many measurement positions in the cell, the calculation of blocking probabilities becomes infeasible. We thus use the well known Kauffman-Roberts recursive formula [15] that calculates rapidly the blocking rates.

#### 2) Dual Carrier

For a cell containing only DC users, the stand-alone throughput is doubled and the cell is viewed as a one queue carrying all the traffic. The CAC condition is thus given by  $\mathbf{m} \cdot \mathbf{c} \leq 2$  and the steady state probabilities become:

$$\pi(\mathbf{m}) = \frac{\prod_{u \in S} \left( \frac{1}{|S|} \frac{E}{2} \right)^{m_u} \frac{1}{m_u!}}{\sum_{\mathbf{m}: \mathbf{m} \cdot \mathbf{c} \leq 2} \prod_{v \in S} \left( \frac{1}{|S|} \frac{E}{2} \right)^{m_v} \frac{1}{m_v!}} \quad (15)$$

The blocking rates can thus be easily solved using the Kaufman-Roberts formula.

#### 3) Mix of single and dual carrier users

When a mix of single carrier and dual carrier users coexist in the cell, the system is again modeled as a network of queues as in Figure 2. This network of queues is now governed by a system of three simultaneous CAC conditions corresponding to the three queues:

$$\begin{cases} \mathbf{m}_1 \cdot \mathbf{c} \leq 1 \\ \mathbf{m}_2 \cdot \mathbf{c} \leq 1 \\ (\mathbf{m}_1 + \mathbf{m}_2 + \mathbf{m}_3) \cdot \mathbf{c} \leq 2 \end{cases} \quad (16)$$

where  $\mathbf{m}_c = (m_{c,u}, u \in S)$  represents the number of users

with radio condition  $n$  in queue  $c$  and  $\mathbf{m} = (\mathbf{m}_1; \mathbf{m}_2; \mathbf{m}_3)$  is the overall system state. We denote by  $\chi$  the set of admissible states verifying the three CAC conditions defined above; the steady state probabilities are thus calculated by:

$$\pi(\mathbf{m}) = \frac{\prod_{u \in S} \left( \frac{1}{|S|} \frac{E_{SC}}{2} \right)^{m_{1,u} + m_{2,u}} \left( \frac{1}{|S|} E_{DC} \right)^{m_{3,u}} \frac{1}{m_{1,u}! m_{2,u}! m_{3,u}!}}{\sum_{\mathbf{m} \in \chi} \prod_{v \in S} \left( \frac{1}{|S|} \frac{E_{SC}}{2} \right)^{m_{1,v} + m_{2,v}} \left( \frac{1}{|S|} E_{DC} \right)^{m_{3,v}} \frac{1}{m_{1,v}! m_{2,v}! m_{3,v}!}} \quad (17)$$

The blocking probability for each queue is then calculated by:

$$b_c = \frac{1}{|S|} \sum_{u \in S} \sum_{\mathbf{m}: (\mathbf{m} + \mathbf{e}_{c,u}) \notin \chi} \pi(\mathbf{m}) \quad (18)$$

where  $\mathbf{e}_{c,u}$  is a vector having 1 in the component corresponding to position  $u$  of queue  $c$  and 0 elsewhere.

Unfortunately, the Kaufman-Roberts formula cannot be used in this case. A conservative bound for the blocking rates is obtained by taking independently each queue  $c$  with its own CAC condition and calculating its blocking rate  $b_c^{ind}$  using Kaufman-Roberts formula. The blocking rates are thus approximated by:

$$\begin{cases} b_1 \approx 1 - (1 - b_1^{ind})(1 - b_3^{ind}) \\ b_2 \approx 1 - (1 - b_2^{ind})(1 - b_3^{ind}) \\ b_3 \approx b_3^{ind} \end{cases} \quad (19)$$

#### 4) Mix of streaming and elastic flows

We finally consider the most general case, where single carrier and dual carrier, streaming and elastic flows share the capacity. As streaming traffic is served first in order to obtain its guaranteed QoS, we use the quasi-stationary assumption and consider that elastic flows receive the average remaining resources, as illustrated in Figure 3.

The average amount of time resources consumed by streaming traffic in both carriers is calculated by:

$$S = \frac{1}{2} \sum_{\mathbf{m} \in \chi} (\mathbf{m}_1 + \mathbf{m}_2 + \mathbf{m}_3) \cdot \pi(\mathbf{m})$$

Elastic flows thus benefit from a single-user throughput equal to  $(1 - S) \cdot T_{alone}(u)$  on each carrier. Their performance can thus be assessed as explained before.

## IV. SIMULATION SCENARIOS AND RESULT

### A. Scenarios and drive test measurements

The measurement campaign has been run in the centre of a major European town. Measurements are available for hundreds of cells, and one typical cell is selected for the capacity calculations (measurement samples are filtered with the scrambling code of the selected cell). This cell is composed of several (non contiguous) parts, which is common in live networks, especially in urban areas, because of irregular propagation from both the serving cell and the many interfering cells around, and because of the irregular cell planning. 1000 measurement samples are available for this cell. The average CPICH Ec/10 on the cell is -7db, and the average CPICH RSCP is -65dBm. The map of the drive test is shown in Figure 4.

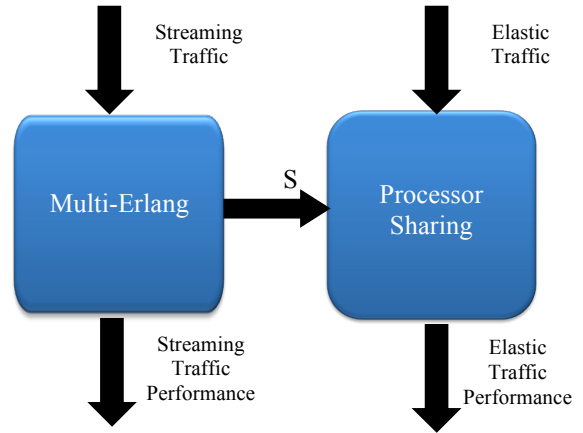


Figure 3. Mix of streaming and elastic traffic.

In order to assess the capacity improvement of HSPA+ dual-cell over the previous HSPA devices, HSPA Release 5 devices have been simulated (categories 12, 6, 8, 9 and 10) as well as HSDPA Release 7 devices (categories 14 and 16) and HSDPA Release 8 (category 20) devices. Simulation parameters are given in Table 1. The symmetrical mode of dual-cell, in which common channels are set on the secondary carrier, is modeled.

PARAMETER	SETTING
Multipath channel	Pedestrian A 3km/h
Orthogonality factor	0,25 for RAKE 0,15 for LMMSE
Downlink interference rise	6 dB
Indoor penetration factor	8 dB
Diversity gain from proportional fair scheduling (PFS)	10%
Diversity gain from PFS in the presence of dual-cell [6]	20%

Table 1: Radio parameters used in the calculations

All the other network settings, that are usually set in simulators as parameters (inter-site distance, antenna gain, path loss model, etc.) do not need to be set in our calculations since they come from the live network.

PARAMETER	SETTING
User throughput target for elastic data services	500 kbps achieved with a 90% probability
Streaming service throughput	250 kbps (5% blocking rate)

Table 2: Parameters used in the capacity calculations

For the sake of simplicity, the main capacity results we present assume that all the devices belong to the same category. Mixes of devices of different categories are then only considered to show the impact of dual-cell devices penetration on the gain. Calculations have been run for streaming traffic, elastic data traffic and a mix of them.

### B. Simulation results and discussion

Single-user throughputs are calculated for all the locations in the cell, for each HSDPA device category. Figure 5 shows the single-user throughput distribution for 21.1 Mbps-capable (category 14) devices. The throughputs are lower than the peak

ones because of the tricky radio propagation conditions, and because of the high inter-cell interference conditions.

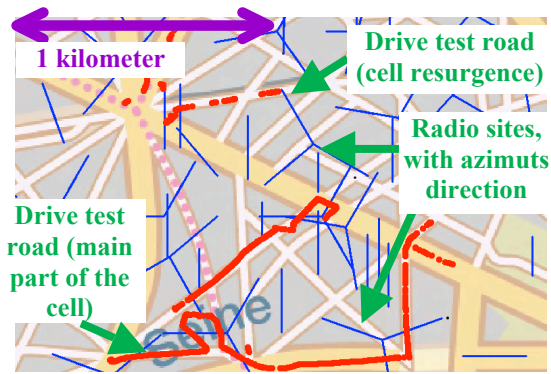


Figure 4. Map of the drive test for the measured cell

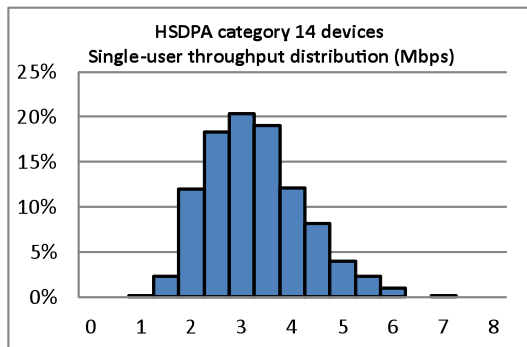


Figure 5. Single-user throughput distribution in a loaded network

Capacity results are given in Figure 6, 7 and 8. It turns out that higher HSDPA mobile categories bring significant capacity improvement over basic ones: from 1.8 Mbps devices to single-cell 42.2 Mbps ones, a  $\times 7$  increase of the cell radio capacity is achieved. The capacity gain from dual-cell (Cat 24) is 38% for streaming services (Figure 6) and 60% for elastic data traffic (Figure 7), which is huge.

Figure 7 shows the impact of a progressive introduction of dual cell devices (Cat 24) in the market, while other legacy devices are supposed from category 14. The capacity, calculated using the model of section III.A.3, increases rapidly until reaching the maximal gain (60%) when dual cell devices become very popular.

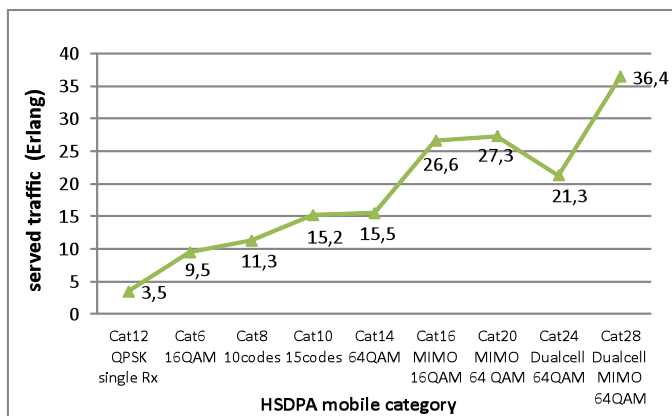


Figure 6. Streaming capacity for all HSDPA device categories (on 10 MHz)

As of Figure 8, it illustrates the capacity of a cell carrying both streaming and elastic users, all equipped with category 24 devices. As streaming calls have priority over elastic ones, the capacity left for data calls reduces when the streaming traffic increases, until reaching almost zero when the streaming traffic attains the cell capacity of 21 Erlangs.

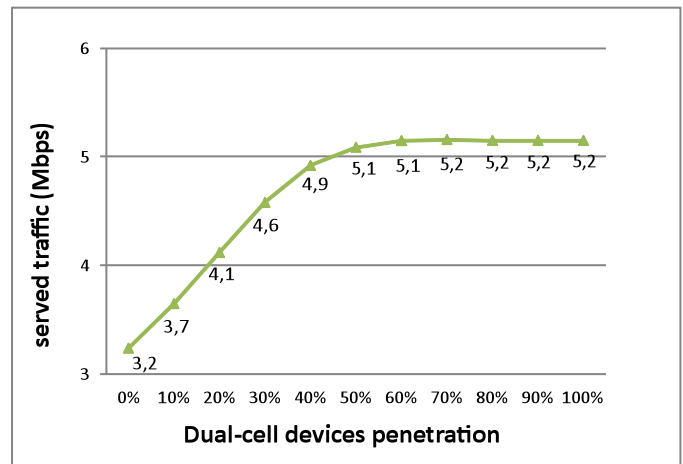


Figure 7. Elastic traffic capacity for different dual-cell devices penetration

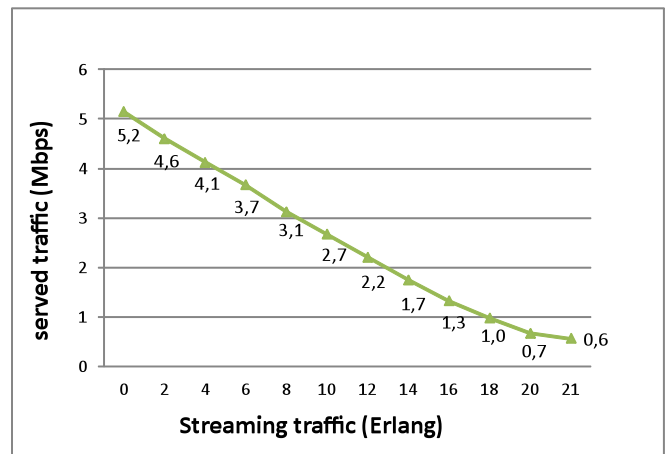


Figure 8. Cell capacity for a mix of streaming and elastic traffic

Note that, from Figure 6, it is obvious that, among the HSPA technology evolutions, those that enhance performance at cell edge also improve significantly the radio capacity. This is true for receive diversity (Cat 6 vs. Cat 12) and MIMO (Cat 16 vs. Cat 10). This is also the case for the dual-cell feature, which provides a twofold improvement of the throughput at cell edge (Cat 24 vs. Cat 14 and Cat 28 vs. Cat 20). The reason is that users at cell edge require an important amount of the shared resources (streaming calls) or stay for a long time in the cell until transferring their files (elastic calls). This is also the reason why 64 QAM does not bring a large capacity gain as it is achieved for a small proportion of users at cell center.

When we compare MIMO with dual cell, the former brings a 95% capacity gain while the latter brings a 45% gain (Figure 6). However, dual-cell has an important advantage over MIMO: it comes only with a software network upgrade, while expensive hardware upgrades are required for MIMO (a new transceiver must be added for each sector). This makes dual-cell more interesting for network operators than MIMO in Release 8, where both features cannot be combined. However,

although MIMO and dual-cell are “competing” features in release 8, they can be combined in Release 9, bringing a combined gain of 150% (Cat 28 vs. Cat 14).

### C. Comparison with other statistical capacity models

In this section, we compare the capacity results obtained with our model with some common models of the literature.

#### 1) Streaming

The classical method for the streaming capacity is to calculate the average throughput over all points of the cell ( $\sum_{u \in S} \frac{T_{alone}(u)}{|S|}$ ) and to use the Erlang-B formula based on the modified admission condition from Eqn. (12):

$$m \leq G_{div} \sum_{u \in S} \frac{T_{alone}(u)}{T^s |S|}, m \text{ being the number of users in the}$$

cell and  $G_{div}$  the diversity gain. Table 3 compares the capacity results for both models. It can be seen that the Erlang B method is optimistic as it does not quantify the impact of cell edge users on capacity.

METHOD	CAPACITY
Erlang B law	25.7 Erlangs for 5% blocking
Model described in III	21.3 Erlangs for 5% blocking

Table 3: Model comparison with Erlang B results. The average throughput over the cell for Cat 24 devices is equal to 7.76 Mbps.

#### 2) Elastic data traffic

The classical measure of network capacity when data calls are considered is the average (arithmetic) cell throughput when several users are served ([7-8]). However, we have shown in [5][10] that the "harmonic mean" of the achievable throughputs gives the maximum traffic the cell can sustain while being stable, but without any QoS guarantee. Indeed, the harmonic mean takes into account the fact that users with bad radio conditions stay longer in the cell and contribute more to the cell load.

Figure 9 compares five capacity measures: the arithmetic and harmonic averages of the throughput (after adding the diversity gain), and the statistical cell capacity when the target throughput is equal to 250, 384 and 500 Kbps. First, we observe that the arithmetic mean over-estimates the capacity. Second, the higher is the target QoS, the lower is the cell capacity. Indeed, all the results from the statistical model are lower than the harmonic mean (that can be considered as the capacity with a target throughput of 0); when the target QoS decreases, the capacity thus gets closer to the harmonic mean.

As of the dual cell gain, the inverse tendency is observed. Indeed, if we focus on dual cell Cat 24 devices and compare them to single carrier ones (Cat 14), the capacity gain is 60%, 46%, and 33% for a target QoS of 500 Kbps, 384 Kbps and 250 Kbps, respectively. The only gain for the harmonic mean is that due to increased diversity gain (10%). This is not surprising since the trunking capacity gain is known to increase when the relative QoS (target QoS divided by the absolute capacity) increases.

## V. CONCLUSION

This paper develops a complete HSPA+ radio capacity model that starts from link level simulations, combines them with drive test measurements, and uses the obtained data rates as an input for a queuing theory model. The results show that the HSPA+ dual cell feature improves the cell capacity significantly (around 40% of additional streaming capacity). This capacity gain increases up to 150% if dual cell is combined with MIMO, using non-linear SIC receivers (both are Release 9 features). Thanks to HSPA+ technology evolution, HSPA networks shall thus be able to successfully face the traffic increase in the upcoming years.

As of future work, our aim is to study the joint scheduling over 4 carriers, proposed in 3GPP Rel. 10. The capacity model proposed in this paper can also be reused for the LTE-Advanced carrier-aggregation feature, also planned in Rel. 10.

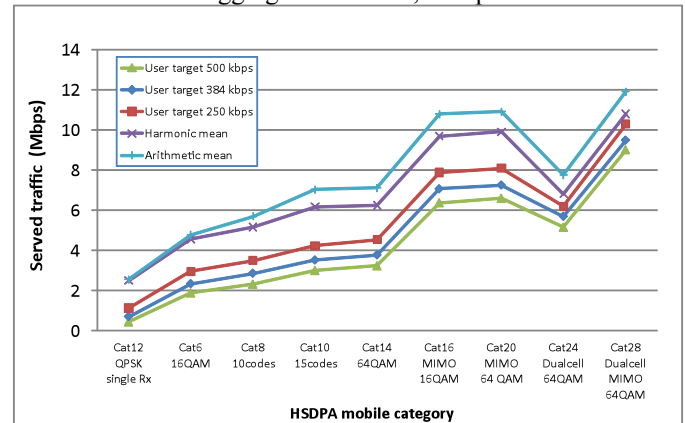


Figure 9. Cell elastic traffic capacity for several QoS targets

## REFERENCES

- [1] 3GPP TS 25.306 V8.7.0, “UE Radio Access capabilities”, release 8.
- [2] 3GPP TS 25.214 V8.6.0, “Physical layer procedures (FDD)”, release 8.
- [3] 3GPP TS 25.306 V9.2.0, “Physical layer procedures (FDD)”, release 9.
- [4] A. Saadani, J.B. Landre, “Realistic Performance of HSDPA Evolution 64-QAM in Macro-Cell Environment”, Proc. IEEE VTC spring 2009.
- [5] T. Bonald, A. Proutiere, “Wireless downlink data channels: User performance and cell dimensioning”, ACM MOBICOM 2003.
- [6] D. Morais, A. Klein, H. Holma, I. Viering, G. Liebl, “Performance evaluation on dual-cell HSDPA operation”, IEEE VTC Fall 2009.
- [7] D. Zhang, P. Kumar, B. Mohanty, J. Hou, “Performance analysis of dual-carrier HSDPA”, Proc. IEEE VTC Spring 2010.
- [8] E. Seidel, J. Afzal, G. Liebl, “Dual cell HSDPA and its future evolution”, White paper, Nomor Research GmbH, January 2009.
- [9] J.B. Landre, A. Saadani, “Receive diversity and LMMSE equalization benefits for HSDPA: Realistic network throughputs”, IEEE PIMRC’07.
- [10] J.B. Landre, A. Saadani, F. Ortolan, “HSDPA radio capacity improvement with advanced devices”, IEEE VTC-spring 2010.
- [11] S. Ghauri, I. Slock, “Receiver designs for MIMO HSDPA”, IEEE ICC’08.
- [12] 3GPP TR 43.030, “Digital cellular telecommunications system (Phase 2+); Radio network planning aspects”.
- [13] H. Holma, A. Toskala, “HSDPA/HSUPA for UMTS: High speed radio access for mobile communications”, Wiley, May 2006.
- [14] T. Bonald, A. Proutière, J. Roberts, J. Virtamo, “Computational aspects of balanced fairness”, ITC 18, 2003.
- [15] J.W. Roberts, “A service system with heterogeneous user requirements”, Performance of Data Communications Systems and Their Applications, North-Holland, Amsterdam, 1981, pp. 423-431.